Segmentation in episodic tremor and slip all along Cascadia

Michael R. Brudzinski and Richard M. Allen

Geology **35** (10) 907-910, 2007, doi: 10.1130/G23740A.1

Data Repository:

Methods for Automated Data Processing and Observations of ETS in Cascadia

A.1. Slow Slip Episodes

In this section, we discuss the relevant information for identification of slow slip episodes, with additional details presented elsewhere (Holtkamp et al., 2006, ms. in prep.). The GPS data analyzed for slow slip episodes is from the PANGA network provided by the Central Washington University clearinghouse (2005). PANGA time series are network solutions with phase ambiguities resolved and typically consist of one sample per day. Provided time series have been postprocessed with GIPSY, and have linear trends, steps due to earthquakes or hardware upgrades, and annual and semi-annual sinusoids signals simultaneously estimated and removed (Szeliga et al., 2004). In this study, the signal to noise ratio of the GPS data is further enhanced by taking a 10 sample running average of the time series that reduces the scatter among neighboring data points.

As shown in previous studies examining transient episodes (Brudzinski et al., 2007; Larson et al., 2004; Lowry et al., 2001), anomalous displacements during slow slip events can be estimated by fitting the GPS coordinate time series with combination of a linear and hyperbolic tangent function. By using a grid search over hyperbolic tangent function parameters (timing and duration of transient), the linear parameters of steady-state velocity and transient displacement are estimated via least squares minimization, weighted by the formal inverse variance of GPS coordinate estimates. This technique has been particularly useful for characterizing the precise timing and overall displacement when a slow slip episode has been identified (Brudzinski et al., 2007; Larson et al., 2004; Lowry et al., 2001).

Slow slip episodes are automatically identified by 1) applying the hyperbolic tangent fit over a scrolling window of the time series (6 months before event time and 6 months after) incremented at 0.01 years, 2) using an f-test to confirm when the combined linear and hyperbolic tangent fit is significantly better than a linear fit at 99% confidence within the window, and 3)

establishing a threshold value for the transient displacement (~2.0 mm) to identify potential events that are larger than background noise from examination of stations within the stable continental interior (DeMets et al., 2004).

Slow slip episodes are verified and event times are selected with an algorithm that first identifies one of the components with an event magnitude that exceeds the displacement threshold and the chi squared value associated with that component must be low. Precise times are selected when the ftest value is near its maximum relative to neighboring times, and the chi squared value is minimized relative to neighboring times. If multiple events within 0.25 years are identified, we take the time with the lowest ratio of the chi squared value to the average chi squared value for all times in the time series. Of these potential events, each one goes through a series of tests (density of data samples, chi squared relative to all time series, and coherence with other neighboring stations) to determine whether it should be included or excluded. Lastly, we perform a manual closer inspection of events, including a handful of extra events that are clear in the time series but only met a smaller displacement threshold (1.5 mm) and excluding a small set of events that appear as noise spikes in the time series. Further details of this analysis will be presented in separate work (Holtkamp et al., 2006, ms. in prep.).

A.2. Non-volcanic Tremor (NVT)

In this section, we discuss the relevant information for identification of episodes of NVT, with additional details presented elsewhere (Brudzinski and Allen, 2006, ms. in prep.). The seismic data for analysis of NVT comes from a variety of networks that spread across the Cascadia subduction zone including the PNSN, USGS-NCSN, CNSN, OATS, IRIS-GSN, BDSN, and the new EarthScope Transportable Array. These networks primarily consist of short period vertical component seismometers, but these are ample instruments to identify NVT which has characteristic frequencies between 1 and 10 Hz (Obara, 2002). Although signals appear to be more pronounced on horizontal components when they are available, vertical components have been sufficient to clearly identify NVT episodes. PNSN data comprise the majority of data analyzed in this study, but continuous data only goes back to 2002, so longer running stations of other networks are critical for identifying longer term trends.

Typically a permanent broadband seismic station uses 24-bit digitizers to continuously record all three components of ground velocity at a rate of 20 samples per second. To fully analyze this voluminous dataset which lasts up to 15 years, we use an automated scheme which begins by

removing the instrument response and applying a filter with a pass-band of 2-6 Hz. We then take absolute values of the time series and calculate the envelope. Up to this point, our analysis is the same as other researchers (Obara, 2002; Rogers and Dragert, 2003; Szeliga et al., 2004). Next, instead of judging whether tremors are present in each segment of data by the hour, we calculate the mean amplitude of the envelope (Figure A1a). Since various non-tectonic factors can influence the amplitude, we limit our analysis to nighttime hours when culture-generated noise is at a minimum and exclude hours during which signals from known, large earthquakes or other spikes, such as those used for instrument calibration, are present (Figure A1b). To further avoid seismic events, we exclude hours with a high max-to-mean ratio. To help reduce longer-term noise trends that exist at a few stations, we high-pass filter the envelope time series to signals with periods less than about a week (Figure A1c). Lastly, we average amplitudes over a four-day moving window to help accentuate sustained tremor activity, and we normalize to values between 0 and 1 (Figure A1d).

In the final time series, large peaks are identified as periods during which tremors dominates. The first cut for identifying NVT periods is by marking peaks that rise above background noise at greater than the 3σ confidence interval. In some cases, analyst intervention is necessary to identify NVT periods due to data loss. To confirm NVT, individual seismograms are investigated as well as mean amplitude time series from neighboring stations.

We also find that in some cases there are peaks that do not meet the 3σ confidence interval threshold, but the timing corresponds to peaks that meet the threshold at neighboring stations. In these cases, we also find that it is typical for this smaller peak to be accompanied by another smaller peak that is close in time. For these situations, we have added a second criteria that can meet the threshold for an event: at least two successive peaks near in time which rise above background noise at greater than 2σ confidence interval. When calculating the recurrence, we take the mean of the times for the smaller peaks that comprise the event. Our rationale for this second criteria is that these cases predominantly occur at stations near the boundary between regions, suggesting they are recording signals from events in neighboring segments.

The technique used here has two distinct advantage over previous analyses: 1) it does not requiring the scientist to examine each record to evaluate whether NVT has occurred and 2) it does not require an array of stations to identify NVT through station coherence. The first advantage results in the ability to automate the process and analyze data over large ranges of

time and location. Nevertheless, in each case of a large peak, individual seismograms have been examined to confirm the presence of NVT. The second advantage is important for investigating NVT in regions where station density is significantly reduced, like central Cascadia.

A.3. Comparison with Previous Studies

In order to confirm the validity of the automated seismic and GPS single-station methods, we compare the results of the techniques in this study with previous identifications of ETS. Figure A2 compares the results from a previous for southern Vancouver Island (Rogers and Dragert, 2003) with analysis from this study for stations ALBH and VGZ. Despite the different analysis approaches, there is one-to-one consistency among identified tremor peaks and slow slip episodes between the two studies. This confirms that for single stations with a low enough noise level, the automated techniques produce results very similar to that of previous studies relying on inspection of a network of observations. These methods are not replacements for network solutions, they are simply used as surrogates to perform a uniform investigation of ETS over the entire subduction zone while network density is still quite heterogeneous.

We also demonstrate the ability to resolve accurate timing of ETS by illustrating our identification of NVT for the early 2003 event in northern Cascadia that has been characterized in previous papers (e.g., Melbourne, 2004). Figure A3 shows a zoomed in time frame for our seismic time series around the 2003 event, with stations plotted according to distance along strike. Our seismic time series show the same progression to the north and south away from the Puget Sound region seen in the previous GPS analyses, demonstrating that our single station data have the resolution to accurate timing of ETS. Furthermore, our data show that the propagation of ETS is somewhat discontinuous, with changes in timing of the maximum NVT activity by 1-2 weeks around 150 km and 310 km. These locations correspond to the northern and southern boundaries of segment C defined from offsets in timing of several months between other ETS episodes (47.5° and 48.4° in Figure 3 of the main text). These offsets in time during the 2003 event reinforce our proposed segmentation boundaries for ETS.

A.4. Observations of Episodic Tremor and Slip in Cascadia

To illustrate the new set of ETS observations in Cascadia, we plot time series for a total of 43 GPS and seismic stations all along the subduction zone (Figures A4-A5). These time series were selected to show an equal mixture of slow slip episode and non-volcanic tremor events over an along-strike station spacing of ~30 km. The coherence in timing between stations in each

segment provide convincing evidence of common recurrence intervals and segmentation of ETS along strike.

Recurrence intervals for each station are calculated from the mean of each interval between times of slow slip or NVT. Then for each segment, we take the mean of all observed intervals for both slow slip and NVT within that segment. Uncertainties on the recurrence shown in Figure 2 are the 1s standard deviation of observed intervals from the mean within that segment.

We have also constructed an animation of ETS occurrence at stations along Cascadia (Figure A6), to help visualize the segmentation of ETS episodes over time and space. The images in this animation color the station symbols by the time since the last ETS event when data is available. The animation progresses from 1997 to 2006 by 5 day increments, and the time differences between different segments can be seen in when a group of stations “reset” to a dark red color. Also, one can begin to see the propagation of ETS onsets during a given event from our dataset.

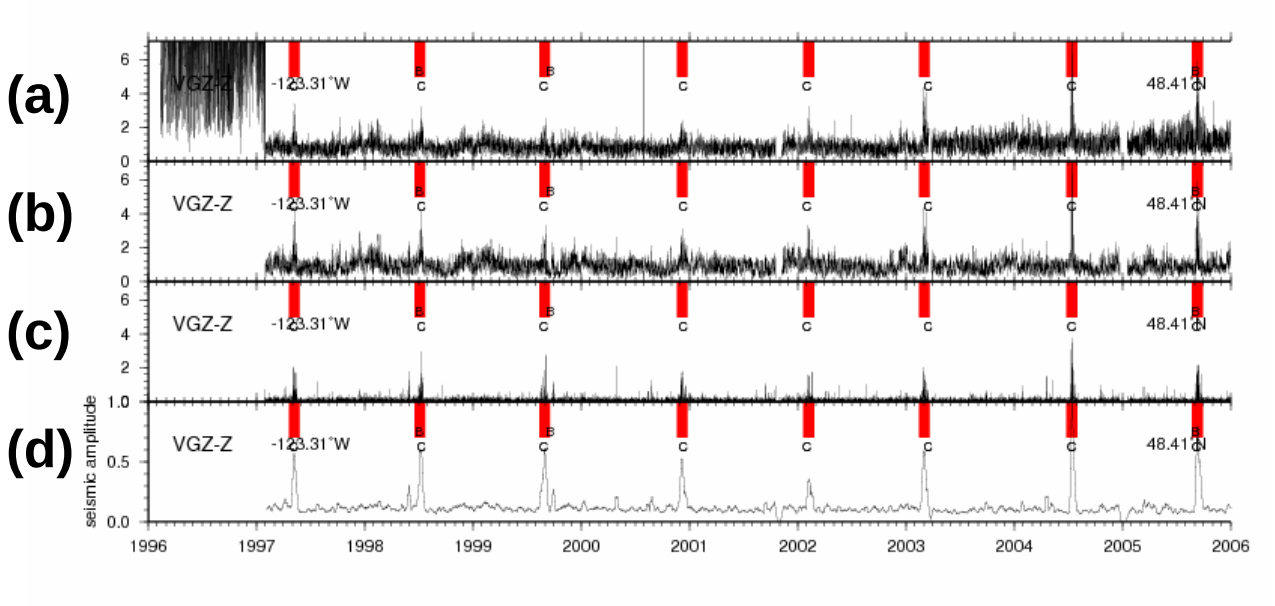

Figure A1. Processed time series for seismic activity at station VGZ on southern Vancouver Island illustrating the effects of different components of our processing. (a) Time series are created by taking the mean amplitude of each hour segment of bandpass filtered envelope seismograms (a). Time series are limited to nighttime hours and those without significant earthquake or instrument glitches (b). Time series are high-pass filtered to amplify signals with periods less than about a week (c). Amplitudes are averaged over a four-day moving window to accentuate sustained tremor activity, and normalized to values between 0 and 1 (d).

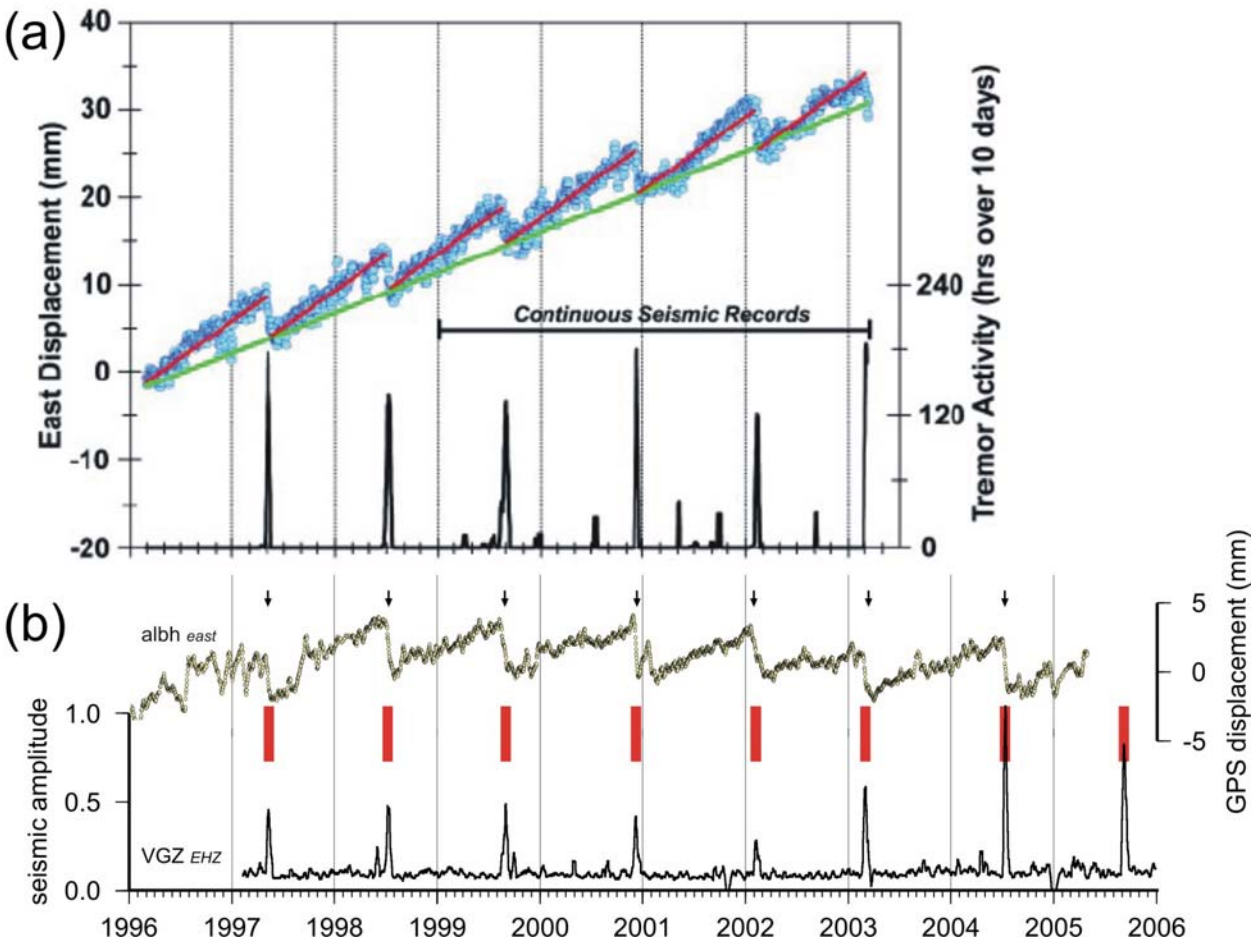

Figure A2. Comparison of slow slip and non-volcanic tremor measurements made in this study with previous analysis of episodic tremor and slip. (a) Plot taken from *Rogers and Dragert* (2003) showing GPS time series for station ALBH relative to North America including both the long-term trend of eastward motions and the slow slip episodes, and hours of tremor activity from a network of seismic stations. (b) Plot showing GPS time series provided by the PANGA network for station ALBH relative to North America with long-term trend removed and stations corrections made. We have further reduced the scatter by using a 10 sample running mean to help accentuate slow slip episodes. Tremor activity is identified for station VGZ by the single-station method of this study. Despite the different analysis approaches, there is one-to-one consistency among identified tremor peaks and slow slip episodes between the two studies.

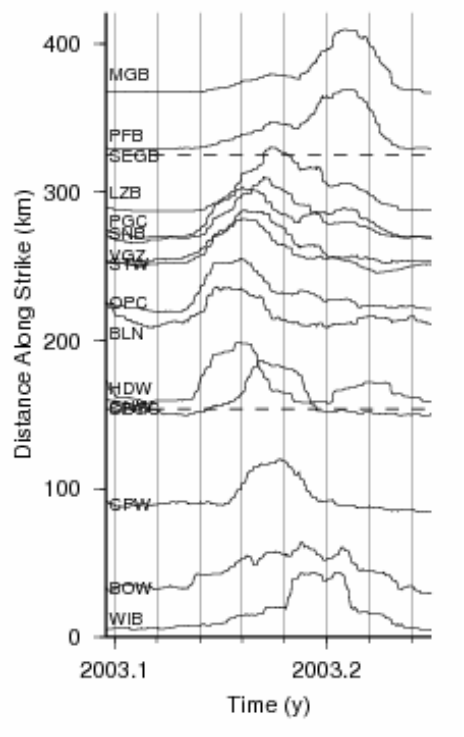

Figure A3. Zoomed view of NVT activity for the 2003 ETS event showing stations from north-central Cascadia plotted according to their distance along strike from the Oregon-Washington border. Distance is estimated by projecting stations onto the 40 km contour of the slab interface. Vertical bars mark week-long increments. Note that the progression to the north and south from the central Puget Sound region is discontinuous, with jumps in timing around 150 km and 310 km. These locations correspond to the northern and southern boundaries of this segment defined from offsets in timing of several months between other ETS episodes (Figure 3, main text).

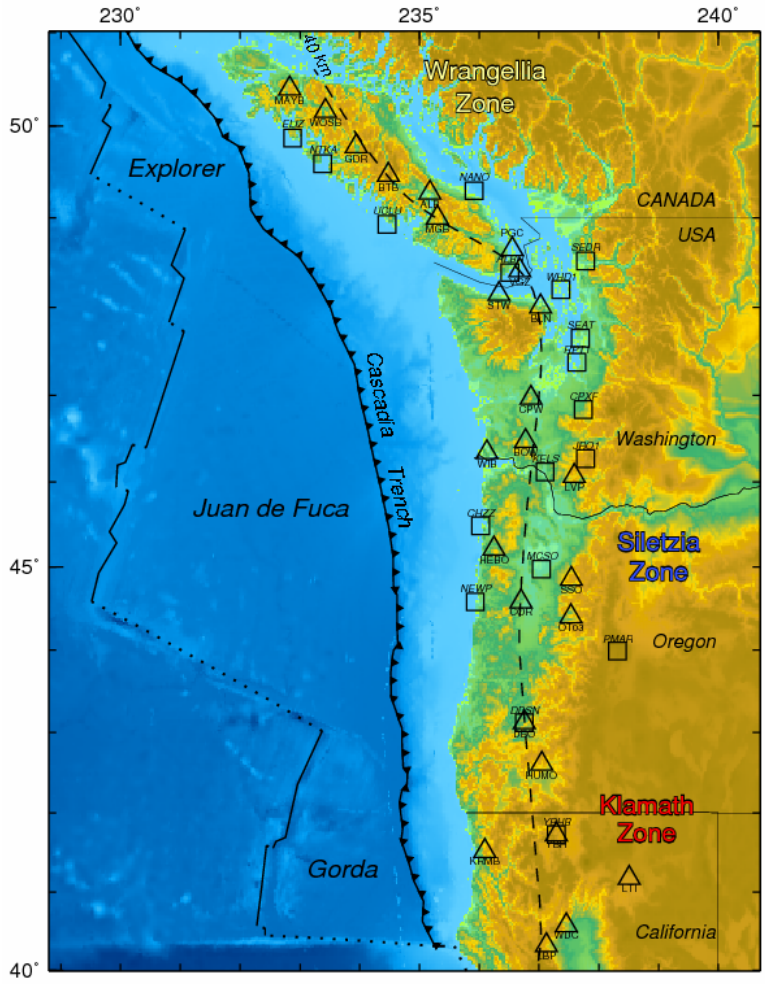

Figure A4. Summary map of seismic (triangles) and GPS (squares) stations in the Cascadia subduction zone whose processed time series and ETS event times are illustrated in Figure A5. The expected source zone is near the dashed 40-km contour of the plate interface.

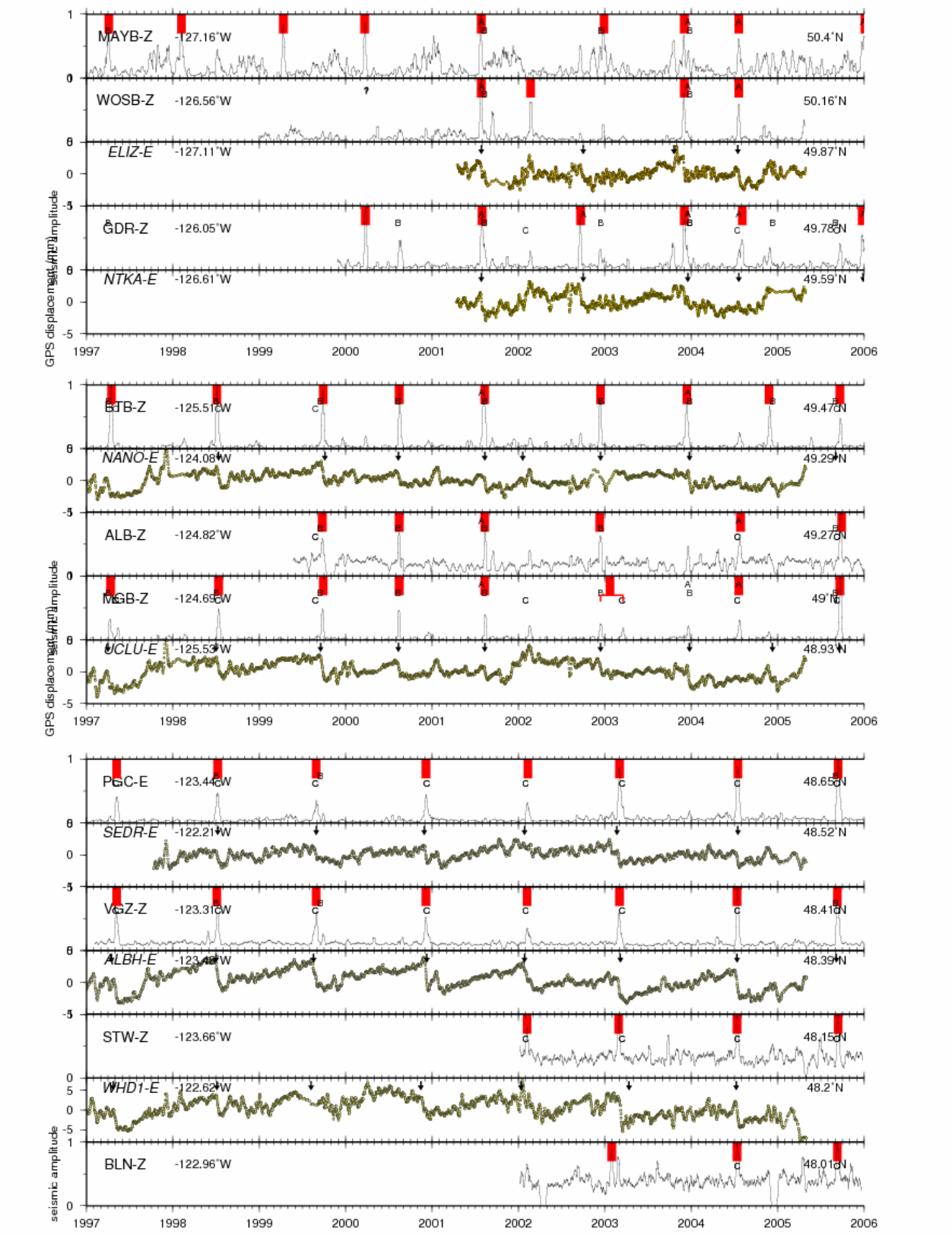
MAYB-Z -127.16°W 50.4°N
WOSB-Z -126.56°W 50.16°N
ELIZ-E -127.11°W 49.87°N
GDR-Z -126.05°W 49.78°N
NTKA-E -126.61°W 49.59°N
BTB-Z -125.51°W 49.47°N
NANO-E -124.08°W 49.29°N
ALB-Z -124.82°W 49.27°N
MGB-Z -124.69°W 49°N
UCLU-E -125.53°W 48.93°N
PGC-E -123.44°W 48.65°N
SEDR-E -122.21°W 48.52°N
VGZ-Z -123.31°W 48.41°N
ALBH-E -123.48°W 48.39°N
STW-Z -123.66°W 48.15°N
WHD1-E -122.62°W 48.2°N
BLN-Z -122.96°W 48.01°N
GPS displacements (cm)
seismic amplitude
1997 1998 1999 2000 2001 2002 2003 2004 2005 2006

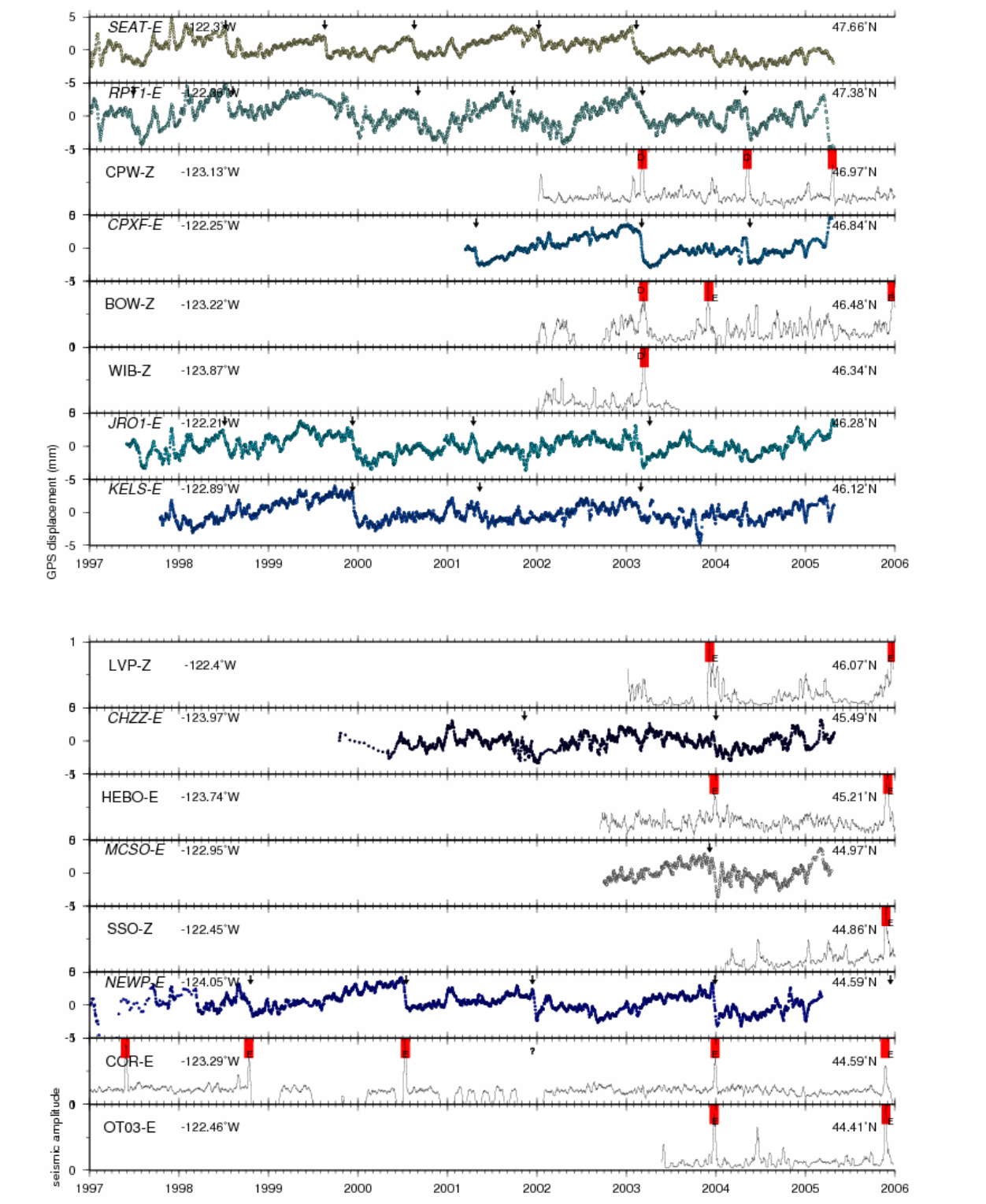
SEAT-E -122.3°W 47.66°N
RPT1-E -122.86°W 47.38°N
CPW-Z -123.13°W 46.97°N
CPXF-E -122.25°W 46.84°N
BOW-Z -123.22°W 46.48°N
WIB-Z -123.87°W 46.34°N
JRO1-E -122.21°W 46.28°N
KELS-E -122.89°W 46.12°N
GPS displacement (mm)
LVP-Z -122.4°W 46.07°N
CHZZ-E -123.97°W 45.49°N
HEBO-E -123.74°W 45.21°N
MCSO-E -122.95°W 44.97°N
SSO-Z -122.45°W 44.86°N
NEWP-E -124.05°W 44.59°N
COR-E -123.29°W 44.59°N
OT03-E -122.46°W 44.41°N
seismic amplitude
1997 1998 1999 2000 2001 2002 2003 2004 2005 2006

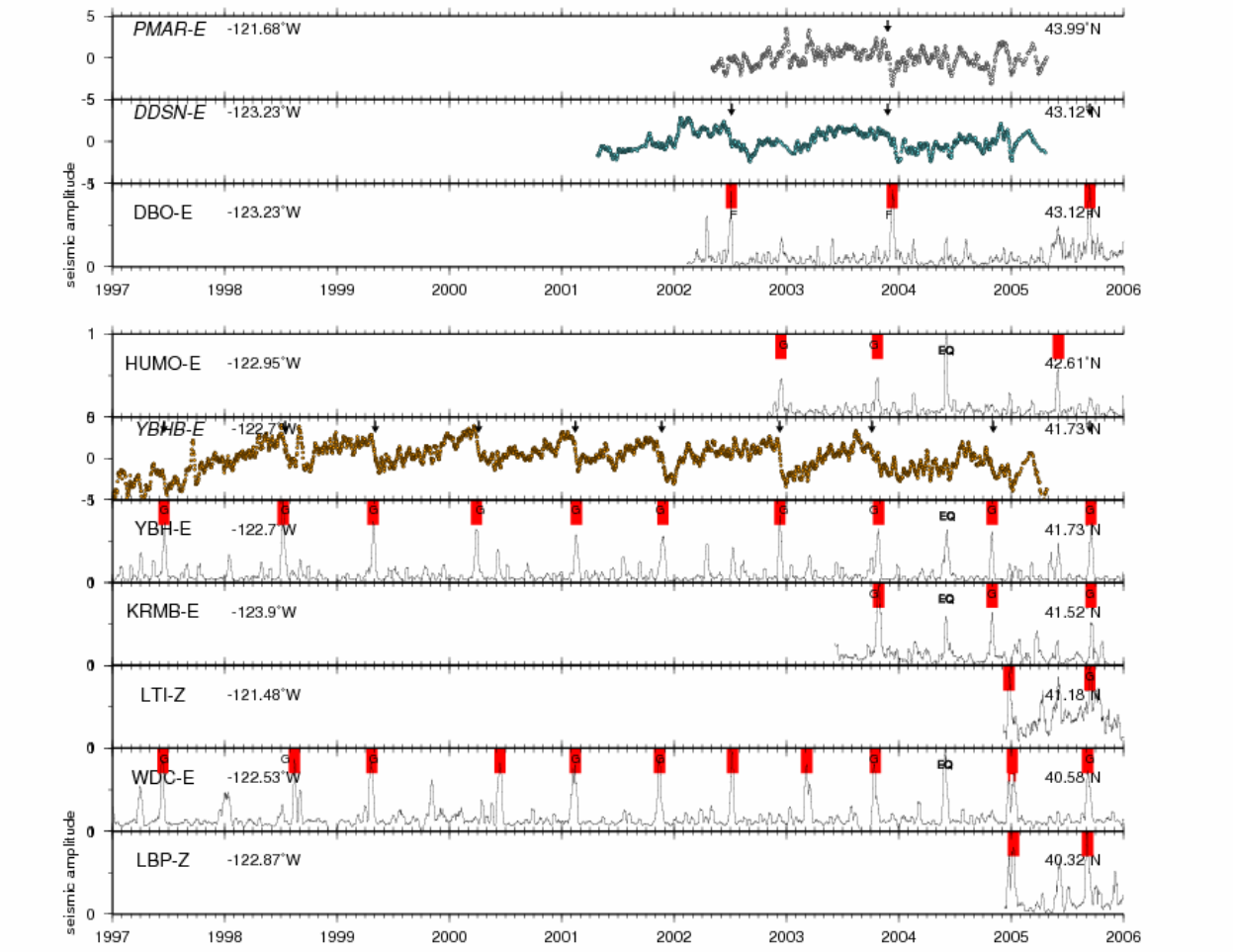

Figure A5. Examples of slow slip and non-volcanic tremor measurements from stations all along the Cascadia margin. Time series and event times are plotted with the same format as Figure 2. Stations are sorted by latitude from the north to the south, separated into the segments of common ETS timing determined in this study. Station locations are shown in Figure A4.

(File: G23740-Brudzinski.figA6.gif)

Figure A6. Animation illustrating ETS occurrence at stations along Cascadia from 1997 to 2006 by 5 day increments, to help visualize segmentation of ETS in time and space. Each image colors stations by time since last ETS event, when sufficient data is available. Time differences between ETS in different segments can be seen when a group of stations “reset” to a dark red color when an ETS event occurs.

References

Brudzinski, M., Cabral, E., DeMets, C., Márquez-Azúa, B., and Correa-Mora, F., 2007, Multiple slow slip transients along the Oaxaca subduction segment from 1993-2006: Geophysical Journal International, p. in review.

Brudzinski, M. R., and Allen, R. M., 2006, Segmentation in Episodic Tremor and Slip All Along Cascadia: Eos trans. AGU, v. 87, p. Abstract T53G-05.

Central Washington University, 2005, Geodesy Laboratory & PANGA Data Analysis Facility, www.panga.cwu.edu.

DeMets, C., Brudzinski, M., Cabral, E., Márquez-Azúa, B., and Correa-Mora, F., 2004, Large-scale seismic and aseismic deformation patterns associated with subduction: Constraints from continuous GPS measurements in Mexico (Abstract): EOS Trans. Am. Geophys. Union, v. 85.

Holtkamp, S., Brudzinski, M. R., and DeMets, C., 2006, Determination of Slow Slip Episodes and Strain Accumulation along the Cascadia Margin: Eos trans. AGU, v. 87, p. Abstract T41A-1541.

Larson, K. M., Lowry, A. R., Kostoglodov, V., Hutton, W., Sanchez, O., Hudnut, K., and Suarez, G., 2004, Crustal deformation measurements in Guerrero, Mexico: Journal of Geophysical Research-Solid Earth, v. 109, p. B04409, doi:10.1029/2003JB002843.

Lowry, A. R., Larson, K. M., Kostoglodov, V., and Bilham, R., 2001, Transient fault slip in Guerrero, southern Mexico: Geophysical Research Letters, v. 28, p. 3753-3756.

Obara, K., 2002, Nonvolcanic deep tremor associated with subduction in southwest Japan: Science, v. 296, p. 1679-1681.

Rogers, G., and Dragert, H., 2003, Episodic tremor and slip on the Cascadia subduction zone: The chatter of silent slip: Science, v. 300, p. 1942-1943.

Szeliga, W., Melbourne, T. I., Miller, M. M., and Santillan, V. M., 2004, Southern Cascadia episodic slow earthquakes: Geophysical Research Letters, v. 31, p. L16602, doi:10.1029/2004GL020824.